

LONGITUDINAL STRIPE OF SORTING NEAR RIPARIAN VEGETATION ZONE

By

Tetsuro TSUJIMOTO

Associate Professor, Department of Civil Engineering, Kanazawa University
2-40-20, Kodatsuno, Kanazawa, 920, Japan

and

Tadanori KITAMURA

Research Assistant, School of Global Environmental Engineering, Kyoto University
Yoshida Honmachi, Sakyo-ku, Kyoto, 606, Japan

ABSTRACT

In a flow with vegetation zone along side wall, the organized turbulence appears. Such an organized motion of fluid is caused by the alternation of the lateral component of the flow velocity with low frequency, whose amplitude is still intense near the channel bed. Hence this organized turbulence influences even the bed-load motion and it brings about alternation of lateral flux of bed-load transport. Since the bed-load intensity in the main channel is obviously higher than that the vegetation zone, the net flux of the lateral bed-load transport is toward the vegetation zone and sediment deposits in the vegetation zone to form a longitudinal sand ridge. When the bed is composed of graded materials, the process accompanies lateral sorting to form a longitudinal stripe of fine sediment. Such a process is investigated in a laboratory flume, and is explained by the non-equilibrium bed-load transport model for each grain size.

INTRODUCTION

Vegetation often exists on a flood plain to provides a riparian habitats. It affects not only flow but also morphological change of a river bed through the change of the sediment transport during floods. The riparian habitat is always disturbed but it would be maintained by the growth of the vegetation in the intervals of floods.

Photo 1 shows an almost straight river with a vegetation zone, which has a longitudinal sand ridge covered by fine materials formed during floods. How was this sand ridge formed, and apparently from sediment transport in a longitudinal direction?

The flow in the vegetation zone during floods is very much retarded. This slower flow in the vegetation zone and the faster flow in the main course influence each other, which causes a lateral flux of momentum and suspended sediment transport. The transverse difference of the lateral flux of sediment promotes the change in the transverse bed profile (Ikeda *et al.* (1, 2)). The lateral mixing contributes to the organized structure of turbulence that has a low frequency fluctuation of velocity associated with the water-surface fluctuation (3~6). Figure 1 demonstrates the measured velocity fluctuation and water-surface fluctuation of the flow with the vegetation zone along side wall of the channel. This velocity fluctuation has a low frequency and it is so intense that it influences even the bed-load motion. This produces an alternation of the lateral flux of the bed-load transport. Since the bed-load intensity in the main course is obviously higher than that in the vegetation zone, the net flux of lateral bed-load transport is toward the vegetation zone and the sediment deposits there to make a longitudinal sand ridge. Tsujimoto & Kitamura (7) observed such a process in a laboratory flume and described it by applying the non-equilibrium bed-load transport model in the lateral direction.

Photo 1 suggests that the longitudinal sand ridge accompanies the lateral sorting of the graded materials, when the bed is composed of graded materials. In this study, lateral sorting process near vegetation zone was surveyed in a laboratory experiment creating an idealized situation. Furthermore, such a process was explained by applying the non-equilibrium bed-load transport model for each grain size.

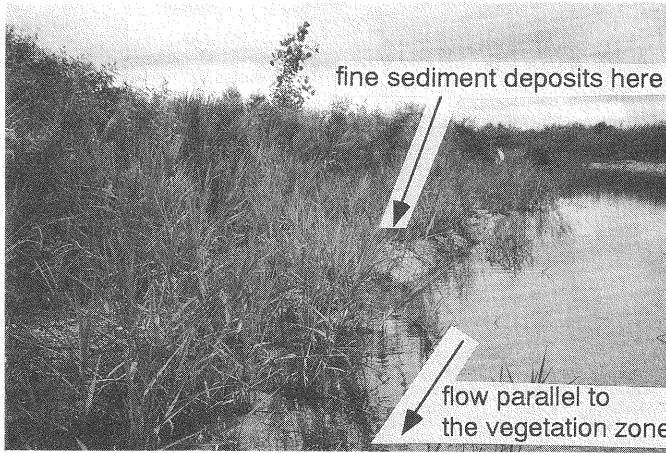


Photo 1 Longitudinal stripe of sorting near vegetation zone in the River Kizu

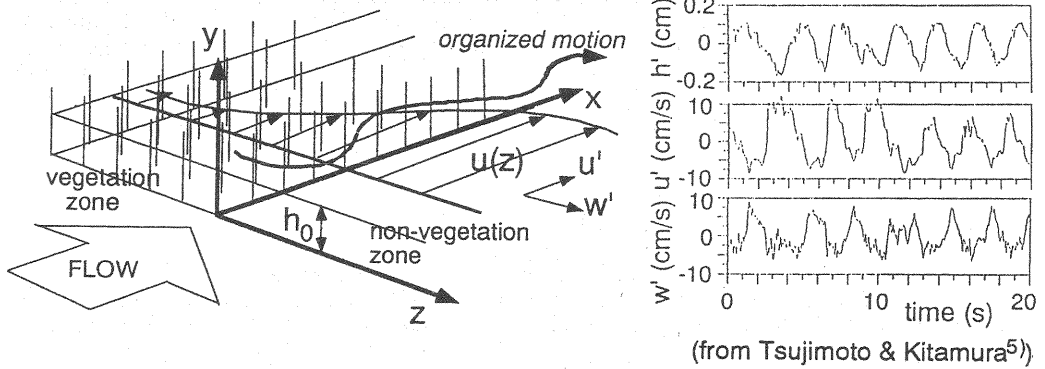


Fig.1 Organized fluctuation appearing in the flow of the vegetation zone

In this study, the vegetation was represented by a group of cylinders with a constant diameter set on the bed distant from each other, and a zone along the side wall of the channel was postulated to be vegetated. When the whole bed was covered by the dense vegetation and the flow depth was smaller than the vegetation height, the characteristic velocity U_{s0} appeared in the vegetation zone proportional to the square root of energy gradient,

$$U_{s0} = K_s \sqrt{I} \quad (1)$$

in which I =energy gradient; and K_s represents the hydraulic characteristics of the vegetation zone. When the group of cylinders represents the vegetation, K_s is given by

$$K_s = \sqrt{2gs^2/(C_D D)} \quad (2)$$

in which C_D =drag coefficient; D =diameter of cylinder; s =interval between the centers of the cylinders and g =gravity acceleration. When the vegetation cover is sparse, the resistance caused by the shear acting on the bed surface is not negligible. In this study, the vegetation cover which was so dense that the effect of the shear was negligible on the resistance in the vegetation zone was treated.

The bed was a graded material constituting of N classes with diameter d_i at the volumetric fraction p_i ($i=1 \sim N$).

FLUME EXPERIMENT

The experiments were conducted in a 12m long, 50cm wide flume. The model vegetation zone was prepared with a group of cylinders ($D=0.25\text{ cm}$, $s=2\text{ cm}$, $K_s=160\text{ cm/s}$); Fig.2 shows their arrangement in the flume. The width of the vegetation zone was 25cm. A length of 3m was prepared as a movable bed made of the mixture, which was composed of a "coarse sand" ($d_1=0.088\text{ cm}$) and "fine sand" ($d_2=0.034\text{ cm}$). The volumetric ratio of the respective sand types to the mixture was set at $p_{10}=p_{20}=0.5$. The coarse sand was colored by green volatile ink to distinguish it from fine sand. The thickness of the movable bed was 4cm, and the movable bed surface had the same level as the rigid bed with glued sand roughness.

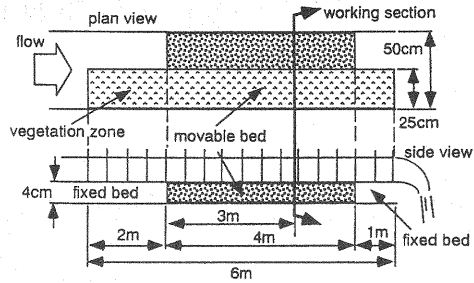


Fig.2 Experimental flume

Table 1 Experimental condition

RUN	d_1 (cm)	d_2 (cm)	p_{10}	i_b	h_0 (cm)	U_{*0} (cm/s)	Ω
RUN 1	0.088	0.034	0.5	1/150	4.0	5.11	0.152
RUN 2	0.088	0.034	0.5	1/300	4.0	3.61	0.152

The depth of flow, h_0 , (before the appreciable bed deformation) was set 4.0cm (smaller than the vegetation height). The experiments were conducted with the same depth but different slope i_b and water discharge, as shown in Table 1, in which $\Omega=C_D D h_0 / (2s^2)$, and $u_{*0}=\sqrt{gh_0 i_b}$. During any experimental run, no sediment was supplied from the upstream sector, and the experiment was finished before appreciable bed degradation was brought about.

At proper time interval to the measurements, the water supply was stopped, then the transverse bed profile was measured and a photo of the bed-surface condition was taken.

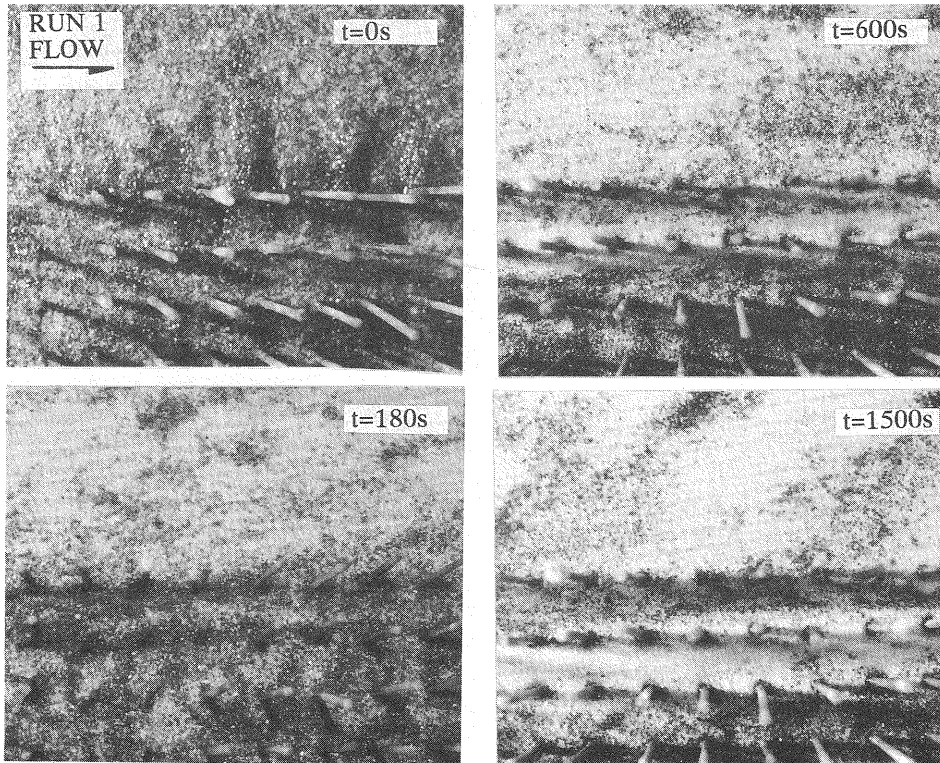


Photo 2 Change of bed-surface condition with time

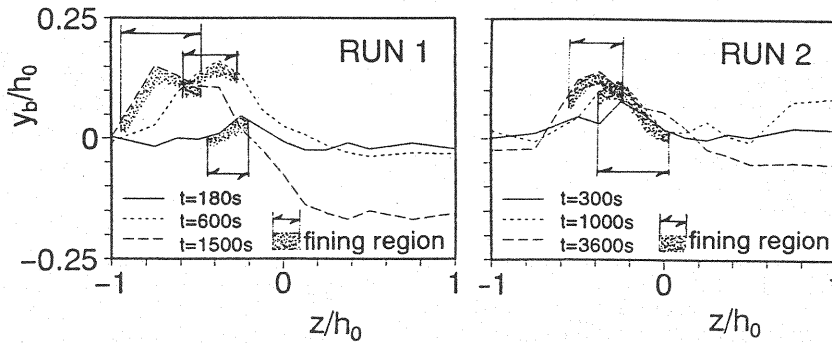


Fig.3 Growth of sand ridge and sorting

Photo 2 shows the change in bed-surface composition with time in RUN 1. An undistinct fine sand stripe had appeared at $t=180s$ (t =time after the introduction of water discharge on the bed), and then it became obvious at $t=600s$. From the photo at $t=1,500s$, the stripe of fine sand shifted toward the inside of the vegetation zone. On the other hand, the gravel sheets (longitudinally alternate sorting) were observed in the main channel after 600s.

Figure 3 shows the temporal change of the transverse bed profile near the boundary of the vegetation zone ($z=0$: boundary of the vegetation zone, $z<0$: vegetation zone, $z>0$: non-vegetation zone), and the figure shows that sand deposition appears near the boundary of the vegetation zone to make a sand ridge. The crest of the sand ridge shifts towards the inside of the vegetation zone with time. In Fig.3, the zone covered by fine sand is indicated as shaded areas. Sand ridge formation as a sorting process can be recognized.

The motion of the sand was in the bed-load and not in the suspended load for any of the experiments, according to our observations. Tsujimoto & Kitamura (7) shows that the organized velocity fluctuation, which is too intense to influence even bed-load motion, appears in the flow with vegetation zone along a side wall, and this velocity fluctuation produces an alternation of the lateral flux of the bed-load. In this experiment, we also observed that the sand moved downstream in a zigzag manner. We believe that it must cause the formation of the sand ridge with sorting.

MODEL FOR TRANSPORT OF GRADED MATERIAL NEAR VEGETATION ZONE

When a stream with a vegetation zone has a movable bed composed of uniform sand, a longitudinal sand ridge is formed near the vegetation zone by lateral transport of the bed-load. This process was explained by applying the non-equilibrium bed-load transport model by Nakagawa & Tsujimoto (8) and was investigated by a flume experiment by Tsujimoto & Kitamura (7). When the bed is composed of graded material, the lateral bed-load transport is different for each size of material, which must have been brought about the sorting. In this study, a non-equilibrium bed-load transport model of graded material was used to explain the formation of a sorting stripe near the vegetation zone, which was successfully applied to describe the armoring, pavement, and both longitudinally alternate and laterally alternate sorting processes (9).

The volumetric ratio of the i -th class of sand with a representative diameter of d_i to the total volume of the surface layer of the bed was represented by p_i , and the pick-up rate and the mean step length of i -th class sand by p_{si} and Δl_i , respectively.

For simplicity, the fluctuation of the lateral component of velocity is approximated as step waves with an amplitude of w_{rms} and a period of ΔT_L , repetition of $+w_{rms}$ and $-w_{rms}$ as shown in Fig.3. The ΔT_L was long enough to affect the bed-load motion. The lateral transport rate of the bed-load for each grain size during the period of $w'>0$ and $w'<0$, $q_{Bzi1}(z)$ and $q_{Bzi2}(z)$ are as follows by applying the non-equilibrium transport formula (9) to the lateral bed-load transport (10).

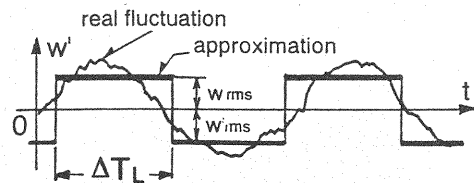


Fig.4 Simplified model of organized fluctuation at a low frequency

$$q_{Bzi1}(z) = \frac{A_3 d_i}{A_2} \int_0^{\infty} \left\{ p_i(z-\zeta) p_{si}(z-\zeta) \exp\left[-\frac{z}{A \sin|\phi_{i1}(z)|}\right] \right\} d\zeta \quad (3)$$

$$q_{Bzi2}(z) = \frac{A_3 d_i}{A_2} \int_0^{\infty} \left\{ p_i(z+\zeta) p_{si}(z+\zeta) \exp\left[-\frac{z}{A \sin|\phi_{i2}(z)|}\right] \right\} d\zeta \quad (4)$$

in which the i indicates the class of sand due to grain size ($i=1, 2, \dots, N$); A_2, A_3 =two- and three dimensional geometrical coefficients for sand; $\phi_{ij}(z)$ =direction of bed-load motion deviated from the longitudinal axis; ρ_0 =porosity of sand; and j indicates the time duration when $w' > 0$ ($j=1$) or $w' < 0$ ($j=2$).

When the bed deformation was negligible, $\phi_{ij}(z)$ is approximated by the flow direction. Hence, when $w_{rms} < U$,

$$|\phi_{ij}(z)| = |\phi(z)| = \frac{w_{rms}(z)}{U(z)} \quad (5)$$

The net lateral transport for each grain size is given as

$$q_{Bzi.net}(z) = \frac{q_{Bzi1}(z) + q_{Bzi2}(z)}{2} \quad (6)$$

The pick-up rate for each grain size, p_{si} , is given by the following formula proposed by Nakagawa *et al.* (12).

$$\frac{p_{si}}{\sqrt{(\sigma/\rho)gd_i}} = 0.03\tau_{*i} \left(1 - \frac{0.7\tau_{*ci}}{\tau_{*i}}\right)^3 \quad (7)$$

in which $\tau_{*i} = u_*^2 / [(\sigma/\rho - 1)gd_i]$; τ_{*ci} =dimensionless critical tractive force for each grain size. When the critical tractive force of sand with d_m ($= \sum [d_i p_i]$) in the mixture is represented by τ_{*cm} ,

$$\frac{\tau_{*ci}}{\tau_{*cm}} = \left(\frac{d_i}{d_m}\right)^\epsilon \quad (8)$$

When $\epsilon = -1$, the difference in the critical shear stress brings about sorting, and, for example, the formation of an armor coat is explained. However, even with $\epsilon = -1$, when there is no difference in critical tractive force for each grain size, sorting is caused by the difference in non-equilibrium transport rate for each grain size (for example, pavement, diffuse gravel sheet, and so on: Tsujimoto (9)). When a part of the bed material moves, $-1 < \epsilon < 0$; while $\epsilon = -1$ when all fractions of bed material moves. In this study, the latter was assumed. Furthermore, τ_{*cm} was here assumed to be identical to the value of the uniform size sand, that is 0.034, according to Iwagaki (13).

On the other hand, the mean step length for each grain size of graded material was assumed to be $\lambda_1 = 20, \lambda_2 = 100$ ($\lambda_{-i} = A_i/d_i$), according to Nakagawa *et al.* (12).

Figure 5 shows the calculated results of q_{Bzi} and $\partial q_{Bzi}/\partial z$. The velocity $U(z)$, the velocity fluctuation $w_{rms}(z)$ and the shear velocity $u_*(z)$ were given according to Tsujimoto & Kitamura (7) (See APPENDIX). Absolute value of $\partial q_{Bzi}/\partial z$ for the fine sand is larger than that for coarse sand near the boundary of vegetation zone within the vegetation zone, which suggests that the deposition of the fine sand is greater than that of the coarse sand. This shows that the sorting stripe appearing near the vegetation is caused by the fact that the net transport rate of bed-load is different to each other.

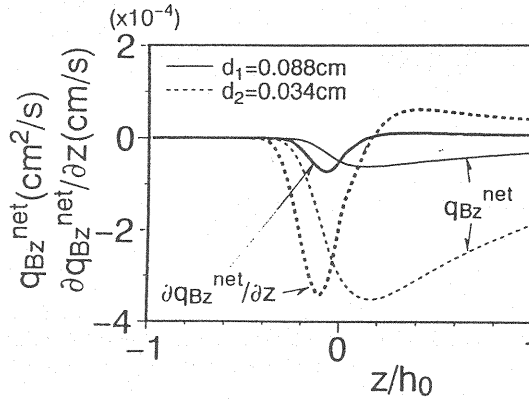


Fig.5 Calculated net lateral transport rate and its derivative with respect to z

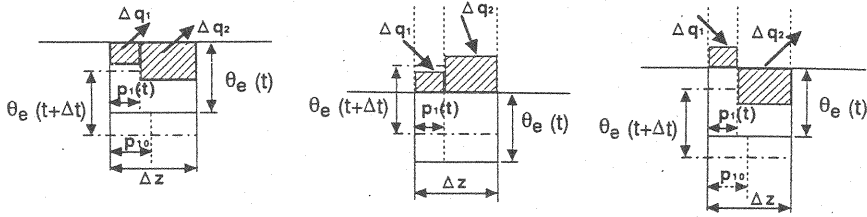


Fig.6 Illustration of mixing model in the exchange layer of the bed surface

SIMULATION OF SORTING PROCESS

Due to the net lateral transport of the bed-load, the apparent volume of i -th class sand depositing during Δt is as follows for unit longitudinal distance;

$$\Delta q_i = - \frac{1}{1-\rho_0} \frac{\partial q_{Bzi}^{net}}{\partial z} \Delta z \Delta t \quad (9)$$

$\Delta q_i > 0$ is the deposition. The change in bed elevation is given by the mass-continuity equation, as follows;

$$\frac{\partial y_b}{\partial t} = \sum_{k=1}^N \frac{\Delta q_k}{\Delta z \Delta t} \quad (10)$$

Figure 6 shows the mixing process of eroded and/or depositing sediment with bed material is illustrated in a simplified mixture composed of two fractions, where p_{i0} = the volumetric ratio of the i -th class sand in the total volume in the substratum (the initial surface layer); θ_e = the thickness of the so-called exchange layer (11); It is here assumed that the thickness of the exchange layer was constant and its order was the maximum size in the mixture. Referring to this figure, the bed-surface composition after Δt is described as follows;

$$p_i(t+\Delta t) = \frac{p_i(t) [\theta_e \Delta z - \sum_{k=1}^N \Delta q_k(t)] + \Delta q_i(t)}{\theta_e \Delta z} \quad (\text{when } \partial y_b / \partial t > 0) \quad ;$$

$$p_i(t+\Delta t) = \frac{p_i(t)\theta_e\Delta z - p_i0 \sum_{k=1}^N \Delta q_k(t) + \Delta q_i(t)}{\theta_e\Delta z} \quad (\text{when } \partial y_b / \partial t < 0) \quad (11)$$

From calculation of the above, Δt should be chosen so as $|\sum \Delta q_k| < \theta_e \Delta z$ and $|\Delta q_i| < \theta_e \Delta z$, and $\Delta q_i = -p_i(t)\theta_e\Delta z$ when $\Delta q_i < -p_i(t)\theta_e\Delta z$, should be assumed.

Figure 7 shows the calculated results on the temporal changes of bed elevation (y_b) and the volumetric ratio of coarse sand (p_1) at several locations of the cross section. To understand the formation of sand ridges and longitudinal sorting, Fig. 8 shows the calculated results expressed as the temporal changes of the profiles of $y_b(z)$ and $p_1(z)$. A sand ridge forms near the boundary of the vegetation zone and develops there. The region where the fine material is greater than the coarse sand appears near the boundary of the vegetation zone, and develops with a shift of location toward the inside of the vegetation zone. These results are consistent to the experimental results shown in Fig. 3.

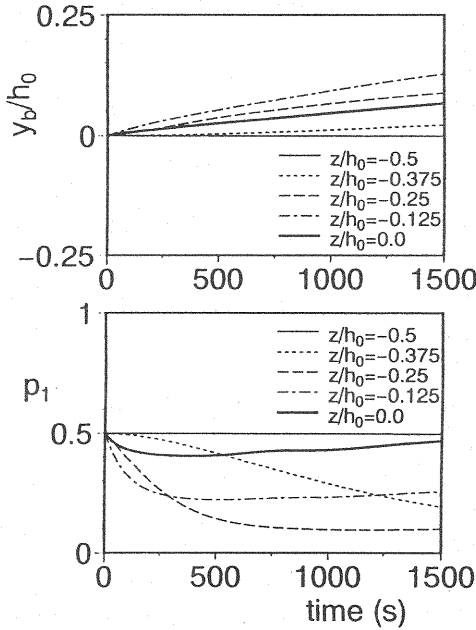


Fig.7 Calculated results on the temporal changes of bed elevation and the volumetric ratio of coarse sand

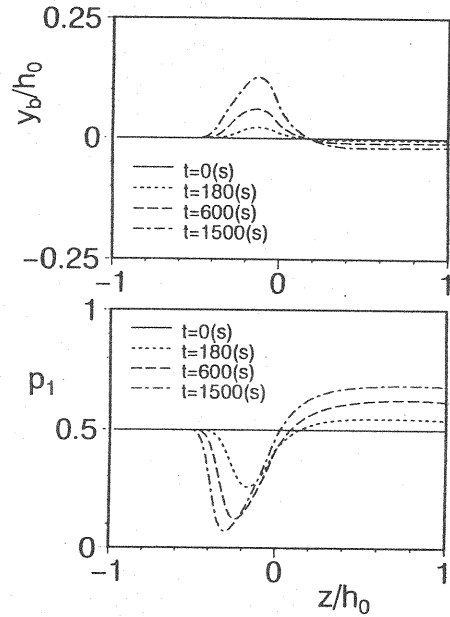


Fig.8 Calculated results of temporal changes of $y_b(z)$ and $p_1(z)$

CONCLUSION

In a laboratory flume, a longitudinal stripe of sorting appeared near the vegetation zone along side wall, resulting from the bed-load motion influenced by the lateral component of the velocity fluctuation. The velocity fluctuation in the flow with the vegetation zone along side wall was so low and the lateral velocity fluctuation so intense even near the bottom that it affected the bed-load motion. The net flux of bed-load in the lateral direction brings a longitudinal sand ridge formation. With bed material of heterogeneous sand, the net fluxes of bed-load for each grain size in the lateral direction were different from each other. Hence the formation of the longitudinal sand ridge accompanies the sorting process. Such a phenomenon was explained by applying a non-equilibrium transport model for each grain size.

APPENDIX

The velocity $U(z)$, the velocity fluctuation $w_{rms}(z)$ and the shear velocity $u_*(z)$ are formulated as follows (a detailed explanation is given in the authors' previous paper (7)).

The following exponential-type distribution was adopted for $U(z)$, which is deduced from an analysis of a horizontal shear flow with a constant eddy viscosity.

$$U^{\#} = 1 + (\sqrt{\gamma} - 1) \exp\left(-\frac{z}{b_m}\right) \quad (z \geq 0) ; \quad U^{\#} = \gamma + (\sqrt{\gamma} - \gamma) \exp\left(\frac{z}{b_s}\right) \quad (z \leq 0) \quad (12)$$

in which

$$\gamma = \frac{U_{s0}}{U_{m0}} = \sqrt{\frac{C_f}{(C_f + \Omega)}} ; \quad \frac{b_m}{h_0} = \sqrt{\frac{\varepsilon_{M*}}{2}} C_f^{-1/4} ; \quad \frac{b_s}{h_0} = \sqrt{\frac{\varepsilon_{M*}}{2}} (C_f + \Omega)^{-1/4} \quad (13)$$

in which $U^{\#} = U/U_{m0}$; $U_{m0} = \sqrt{1/C_f} u_{*0}$ = flow velocity in main course unaffected by vegetation zone; C_f = resistance coefficient of main course; b_m , b_s = effective width of shear flow regions in main course and that in vegetation zone, respectively; $\varepsilon_{M*} = \varepsilon_M/(u_{*0} h_0)$; and ε_M = kinematic eddy viscosity.

The shear velocity is given as follows:

$$u_*(z) = C_f U(z) \quad (14)$$

Ikeda *et al.* (2) assumed the following equation to evaluate the kinematic eddy viscosity.

$$\varepsilon_{M*} = \frac{f(1-\gamma)(b_m + b_s)}{\sqrt{C_f} h_0} \quad (15)$$

in which f is an empirical parameter, often termed the "mixing coefficient." The f value was shown by Ikeda *et al.* (2) written as follows:

$$f = 0.035 \exp[-2.95 \exp(-3.8\gamma)] \quad (16)$$

The amplitude of the transverse velocity fluctuation at the interfacial boundary of the vegetation zone w_0 is related to the f value by the analysis of the lateral mixing of the momentum at the interfacial boundary of the vegetation zone.

$$w_0/U_{m0} = \pi e(1-\gamma) f \quad (17)$$

One can expect that $w_0 \approx w_{rms}(0)$. The lateral distribution of w_{rms} is approximated by the following equations according to the experimental results.

$$w_{rms}(z) = \begin{aligned} &w_{rms\infty} + [w_{rms}(0) - w_{rms\infty}] \exp[-(z/b_m)^2] & (z \geq 0) \\ &w_{rms}(0) \exp[(z/b_s)^2] & (z \leq 0) \end{aligned} \quad (18)$$

in which $w_{rms\infty}$ = the value of w_{rms} in main course unaffected by vegetation ($w_{rms\infty} \approx \sqrt{C_f} U_{m0}$).

REFERENCES

1. Ikeda, S., N. Izumi and R. Ito : Effects of Pile Dikes on Flow Retardation and sediment Transport, *Jour. of Hydraul. Eng.*, ASCE, Vol.117, No.11, pp.1459-1478, 1991.
2. Ikeda, S., K. Ohta and H. Hasegawa : Effect of bank vegetation on flow and sediment deposition, *Jour. of Hydraulic, Coastal and Environmental Engineering*, JSCE, No.447/II-19, pp.25-34, 1992(in Japanese).
3. Fukuoka, S. and K. Fujita : Hydraulic effects of luxuriant vegetations on flood flow, *Rep. Public Works Res. Inst.*, Ministry of Construction, Japan, No.180, pp.129-192, 1988 (in Japanese).

4. Tsujimoto, T. : Spectral analysis of velocity and water-surface fluctuations appearing in an open channel with vegetated and non-vegetated regions in a cross section, *Proc. 6th Int. Sym. Stochastic Hydraulics*, Taipei, R.O.C., pp.197-212, 1992.
5. Tsujimoto, T. and T. Kitamura : Experimental study on open-channel flow with vegetated zone along side wall - Correlative structure of fluctuations of velocity and free surface, *KHL Commun.*, Kanazawa Univ., Vol.3, pp.21-35, 1992.
6. Tsujimoto, T. and T. Kitamura : Appearance of organized fluctuations in open-channel flow with vegetated zone, *KHL Commun.*, Kanazawa Univ., Vol.3, pp.37-45, 1992.
7. Tsujimoto, T. and T. Kitamura : Lateral bed-load transport and sand-ridge formation near vegetation zone in an open channel, *Jour. of Hydrosience and Hydraulic Engineering*, JSCE, Vol.13, No.1, pp.35-45, 1995.
8. Nakagawa, H. and T. Tsujimoto : Sand bed instability due to bed load motion, *Jour. Hydraul. Div.*, ASCE, Vol.106, HY12, pp.2029-2051, 1980.
9. Tsujimoto, T. : Fractional transport rate and fluvial sorting, *Proc. Grain Sorting Seminar*, Ascona, Switzerland, VAW-ETHZ, 117, pp.227-249, 1992.
10. Nakagawa, H., T. Tsujimoto and S. Murakami : Non-equilibrium bed load along side bank, *Proc. 3rd Int. Sym. River Sedimentation*, Jackson, Mississippi, USA, pp.1029-1065, 1986.
11. Parker, G. : Some random notes on grain sorting, *Proc. Grain Sorting Seminar*, Ascona, Switzerland, VAW-ETHZ, 117, pp.19-76, 1992.
12. Nakagawa, H., T. Tsujimoto and S. Nakano : Characteristics of sediment motion for respective grain size of sand mixtures, *Bulletin, Disas. Prev. Inst.*, Kyoto Univ., Vol.32, pp.1-32, 1982.
13. Iwagaki, Y. : Hydrodynamic study on critical tractive force, *Proc. JSCE*, No.41, pp.1-21, 1956(in Japanese).
14. Tsujimoto, T., T. Kitamura and H. Nakagawa : Lateral bed-load transport and sorting near vegetation zone along side wall, *Jour. of Hydraulic, Coastal and Environmental Engineering*, JSCE, No.503/II-29, pp.99-108, 1994(in Japanese).
15. Tsujimoto, T., T. Kitamura and H. Nakagawa : Longitudinal stripe of sorting along vegetation zone in open channel, *Proc. of Hydraulic Engineering*, JSCE, Vol.38, pp.665-670, 1994(in Japanese).

APPENDIX - NOTATION

The following symbols are used in this paper:

A_2, A_3	= two- and three dimensional geometrical coefficients for sand;
b_m, b_s	= effective width of shear flow regions in main course and that in vegetation zone;
C_D	= drag coefficient of vegetation;
C_f	= resistance coefficient of main course;
D	= diameter of cylinders;
d_i	= sediment diameter of i -th fraction sand;
d_m	= mean diameter of sand mixture;
f	= mixing coefficient;
g	= gravity acceleration;
h_0	= mean water depth;
I	= energy gradient;
i_b	= longitudinal bed slope;
K_s	= proportionality constant;
p_i	= volumetric ratio of the i -th fraction sand to that of sand of all fractions in exchange layer;
p_{i0}	= initial value of p_i ;
p_{si}	= pick-up rate (probability density per unit time for a sand particle to be dislodged) for the i -th fraction sand;
q_{Bzi}	= lateral component of non-equilibrium bed-load transport rate for the i -th fraction sand ;
q_{Bzi}^{net}	= net lateral transport rate of bed-load for the i -th fraction sand;
s	= interval between the center of cylinders;
t	= time;
U	= mean primary velocity (depth averaged value);
$U_{\#}$	= dimensionless mean primary velocity (depth averaged value);
U_{m0}	= mean primary velocity in main course unaffected by vegetation zone;

U_{s0}	= characteristic velocity in vegetation zone;
u^*	= shear velocity;
u^*_0	= shear velocity in main course unaffected by vegetation zone;
u_{rms}, w_{rms}	= standard deviation of longitudinal and lateral components of velocity;
w_0	= amplitude of the velocity fluctuation;
$w_{rms\infty}$	= depth averaged value of w_{rms} in main course unaffected by vegetation zone;
x, y, z	= longitudinal, vertical, lateral coordinates;
y_b	= elevation of bed;
ΔT_L	= period of low frequency fluctuation;
Δt	= time step for numerical simulation;
Δz	= transverse distance for numerical simulation;
Δq_i	= deposition rate in Δt and Δz ;
ε	= constant;
ε_M	= kinematic eddy viscosity;
ε_{M^*}	= dimensionless kinematic eddy viscosity;
ϕ_i	= deflection angle of trajectory of bed-load particle against x axis for i -th fraction sand;
γ	= ratio between characteristic velocity in vegetation zone and mean primary velocity in main course unaffected by vegetation zone;
Λ_i	= mean step length of bed-load motion for i -th fraction sand;
θ_c	= thickness of exchange layer;
ρ	= mass density of water;
ρ_0	= porosity of sand;
σ	= mass density of sand;
τ^*_i	= dimensionless tractive force for i -th fraction sand;
τ^*_{ci}	= dimensionless critical tractive force for i -th fraction sand;
τ^*_{cm}	= dimensionless tractive force in main course unaffected by vegetation zone;
Ω	= dimensionless vegetation density; and
ζ	= distance along z axis.

(Received January 26, 1996; revised September 28, 1996)